Sigma Journal of Engineering and Natural Sciences
Web page info: https://sigma.yildiz.edu.tr
DOI: 10.14744/sigma.2025.00159

Research Article

Designing of triple rings metasurface based perfect absorber for C–band and X–band applications

Jigar M. PATEL[1], Rahul D. MEHTA[2,*]

[1]*Department of Electronics & Communication Engineering, Government Engineering College, Gandhinagar Gujarat Technological University, Gujarat, 382424, India*
[2]*Department of Electronics & Communication Engineering, Government Engineering College, Rajkot, Gujarat Technological University, Gujarat, 382424, India*

ARTICLE INFO

Article history
Received: 20 May 2024
Revised: 18 July 2024
Accepted: 22 October 2024

Keywords:
Absorption; C- band and X – band; Metasurface; Perfect Absorber; Triple Circular Ring

ABSTRACT

The present investigation aims to design, simulate and fabricate Triple Rings Metasurface-based Perfect Absorber for C – band and X–band applications. The proposed structure is designed and simulated in CST Simulator software and fabricated hardware of 6x6 array and 10x10 array with the unit cell size 9x9 mm. In simulated results, the maximum absorption for unit cells is achieved for normal EM waves of 96.62% at 7.97 GHz frequency. For the 6x6 Array, the maximum absorption is achieved at 99.04 % and 99.21% at 9.87 GHz and 11.58 GHz respectively with the substrate's thickness of 1.8 mm. For the 6x6 Array, the maximum absorption is achieved at 97.82% at 7.83 GHz respectively with a substrate thickness of 0.8 mm. For the 10x10 Array, the maximum absorption is achieved at 99.04 % and 99.21% at 9.87 GHz and 11.58 GHz respectively with the substrate's thickness of 1.8 mm. For the 10x10 Array, the maximum absorption is achieved at 92.49% at 10.84 GHz with a substrate thickness of 0.8 mm. The proposed structure is investigated by varying the substrate's thickness and the rings' variation. The experimental results show maximum absorption in the C – and X – bands. Due to these results, the proposed design will be used for C–band and X–band applications.

Cite this article as: Patel JM, Mehta RD. Designing of triple rings metasurface based perfect absorber for C–band and X–band applications. Sigma J Eng Nat Sci 2025;43(5):1701−1711.

INTRODUCTION

Recent years have witnessed a lot of work on the design and investigation of metamaterial absorbers for their interesting electromagnetic features and application prospects in C, X, Ku, L, and S-band frequencies. Metamaterial absorbers are absorbers whose structures are designed and can absorb electromagnetic waves fully, therefore have been applied in EMI shielding, stealth technology as well and energy harvesting.

In the year 2023, Patel and Mehta proposed a comparative review on metasurface-based perfect absorbers, where the researchers mainly focused on the performance of the metasurfaces through simulations.[1] An X-shaped triple

*Corresponding author.
*E-mail address: rdmehta@hotmail.com

This paper was recommended for publication in revised form by Editor-in-Chief Ahmet Selim Dalkilic

Published by Yıldız Technical University Press, İstanbul, Turkey

split ring resonator metamaterial absorber is designed and analysed for the quad-band insensitivity of the incidence and polarization angles by Jahan et al. [2], for C, X, and Ku bands. More progress was shown by Jahan et al. [3] with a quad-band metamaterial perfect absorber with a double X-shaped ring resonator for having high shielding effectiveness.

Also, in Ullah et al. [4], 2024, we have a four-band compact metamaterial absorber for electromagnetic energy harvesting application and a metamaterial absorber with triple band microwave proposed by Hossain et al. [5] which uses double E-shaped symmetric split ring resonators for EMI shielding with stealth application. Liu et al. [6]added to designing an ultra-thin absorber with fragmented magnetic structures for L, S, and part of C bands.

Shahid et al.[7] and Rajyalakshmi et al. (2023) designed MMAs for L, S and C bands with particular attention made on the angle dependency [8-10]. Some of the other important contributions are on polarization-independent, wide-angle, broadband metasurface absorber by Amer et al. [11], 2022 using Resistor Loaded Split Ring Resonator and on Dual-band metamaterial for 5G sub-6GHz by Hasan et al. [12] 2022.

Specifically, Hakim et al. [13] presented a detailed study of dual and quad-band metamaterial absorbers for K and Ku [14] bands sensing applications and Kaur & Singh [15] reported a compact ultrathin polarization- and Incident angle -Independent triple band Metamaterial absorber. Deng et al. [16] paid attention to the ultrathin and tri-band MMAs with WIAA for conformal usages in X and Ku bands.

Zhao et al. [17] investigated the features of a V-shaped metamaterial absorber and its possible uses and Singh and Gupta [18] designed a wrenched-square shaped polarization insensitive and wide angle stable ultra-thin metamaterial absorber for S, X and Ku band usages. Finally, Naqvi et al. [19] designed a new meander line metamaterial absorber for 5G at 24 GHz and 28 GHz.

Shakiba et al. [20] introduced a novel, wide operating frequency, multiband PMA that incorporated the switching functionality of phase change materials for biosensing. Tunability and high absorption efficiency of the structure over multiple bands is because of the employment of PCMs which make the absorber suitable for precise biosensing application. As has been pointed out in the given research, metamaterial absorbers have demonstrated promising development in medical and environmental applications.

S, C and X band metamaterial absorber is presented by Afsar et al. [21] which is designed based on one of the fundamental symmetries of the solar system, rotational symmetry. Moreover, due to the helix structure of the proposed design, the efficiency of the power absorption is optimized for wireless communication and the EMI shielding with near-perfect power absorption is confirmed by the simulation and the experiment. Therefore, the study shows the absorber's suitability for effective and consistent electromagnetic wave absorption in communication systems and stealth technologies.

Still, there are some open questions that one has to pose to further improve the concept and application of metamaterial absorbers. Different design solutions can provide multi-band absorbing properties; however, to design an object that gives the true wideband absorbing characteristics over a wider range of frequencies, additional studies are to be made to increase overall flexibility and usability. In a similar regard, recently angle-independent and polarization-insensitive absorbers have also been implemented, however, more enhancements are required to render functionality invariant to operation conditions. Forming very thin layer geometries that still exhibit high absorption efficiency, conformal, and flexible is still a problem, important for integrating technologies into clothing and intricate structures. This is in terms of new materials and techniques of manufacture that are also much more efficient and less expensive but which offer these performances consistently.

DESIGN AND SIMULATION

Design

The basic structure of the Meta surface based on a perfect absorber is shown in Figure 1. The transmitted EM wave (Et) will not pass due to the absorbing nature of the metamaterial. Also, there is no reflection of the EM wave (Er). When reflected power and transmitted power have been minimized simultaneously, absorptivity will be maximum.

The simulation performed using CST software incorporating electromagnetic simulation with frequency solver enables the calculation of absorbance ($A(\lambda)$) from S-parameter results obtained. Thus, for this particular design where a full metal layer is used, the analysis reduces to $A(\lambda) = 1 - |S_{11}|^2$ [1].

For metasurface based perfect absorber, the resonant condition should be matched which is interaction between the thickness of substrate and triple ring structure. The relation between these parameters is shown as below:

$$2\eta_{eff} t_s = m\lambda \quad (1)$$

Where η_{eff} is effective refractive index of the substrate, ts is the thickness of substrate, λ is the wavelength and m are the order of resonance.

If a thick substrate is used, the optical path length for reflected waves will increase and might lead to a change in resonance wavelength. However, a thicker substrate can support several resonant modes — higher orders m, corresponding to multiple absorption peaks. The thickness of the substrate plays a critical role for realizing effective impedance matching between the metamaterial and free space.

In metasurface, absorption $A(\lambda)$ is also a function of the impedance matching between the metamaterial and free space. The reflection coefficient $R(\lambda)$ is related to the impedance mismatch:

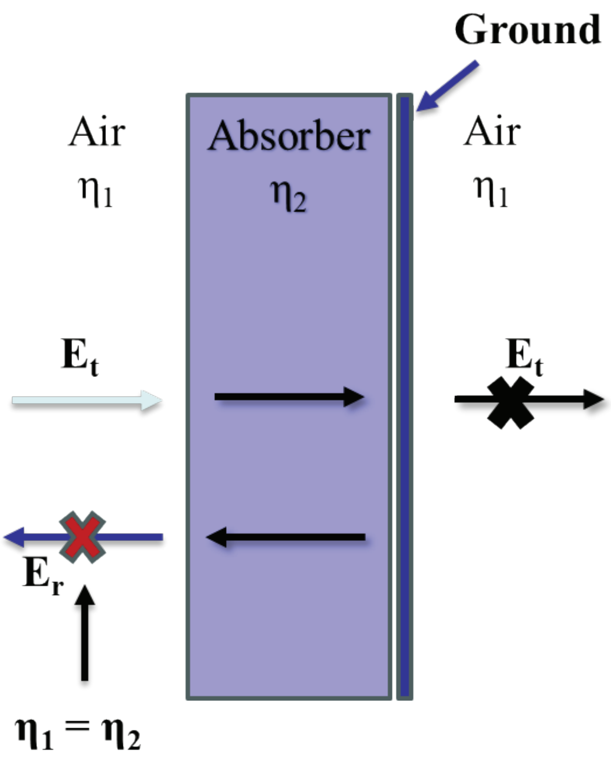

Figure 1. The structure of metasurface absorber.

A triple circular ring metamaterial structure with a circular ring topology is depicted in Figure 3 to demonstrate the structure construction. The physical form of the substrate used for the structure is FR4 and has a dielectric constant of 4.6 and a loss tangent of 0.019. A diagram illustrating one possible metamaterial unit cell suggested for the design is shown below. It is made up of two metallic laminae separated by a dielectric lamina. The topmost metallic layer is constructed using three circular rings with different radii and widths for the triple resonance copper. These rings are spaced by two distinct gaps and both are individually tailored through full wave optimization. The ground plane is made of copper and is connected throughout the device from the lowest metallic level. The substrate dimensions of the unit cell are 9 mm X 9 mm X 0.8 mm in the x direction, y direction and thickness, respectively., where the radii of the circular rings denoted by are 2.33 mm, 2.78 mm, and 3.29 mm, respectively, which plays an important role in the electrical resonance. The widths of the rings are 0.28 mm for the first two and the third one a little bit smaller – 0.26. The first gap is 0.23 mm and the second one is 0.17 mm corresponding to the two rings. One at a time the rings are inserted – inner ring, middle ring and outer ring as illustrated in Figure 4, Figure 5 and Figure 6 respectively.

$$R(\lambda) = \left| \frac{Z_{eff} - Z_0}{Z_{eff} + Z_0} \right|^2 \tag{2}$$

In other terms,

$$A(\lambda) = 1 - \left| \frac{Z_{eff} - Z_0}{Z_{eff} + Z_0} \right|^2 \tag{3}$$

For perfect absorption, Z_{eff} should be matched with Z_0.

The basic block diagram of metasurface based perfect absorber is shown in Figure 2 which shows the basic design of the absorber. Based on this, the first structure is designed which is shown in Figure 3 which contains the three circular rings, made of copper material at top, FR4 dielectric material at middle layer and Copper material at bottom layer.

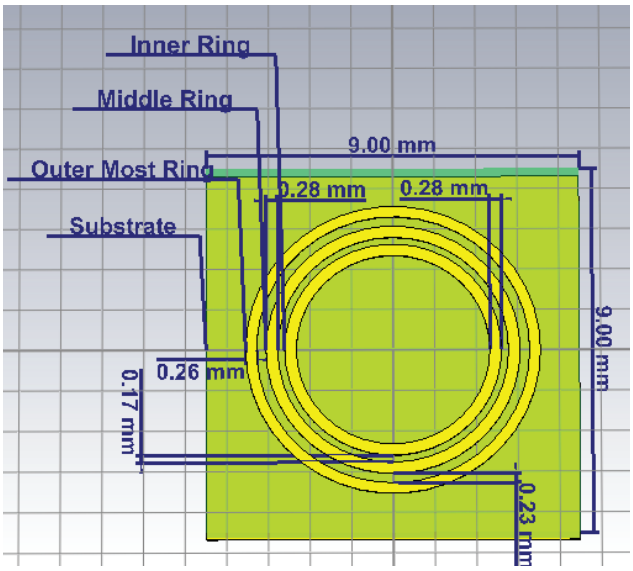

Figure 3. Design: 1 The geometry of the unit cell of the proposed metamaterial absorber.

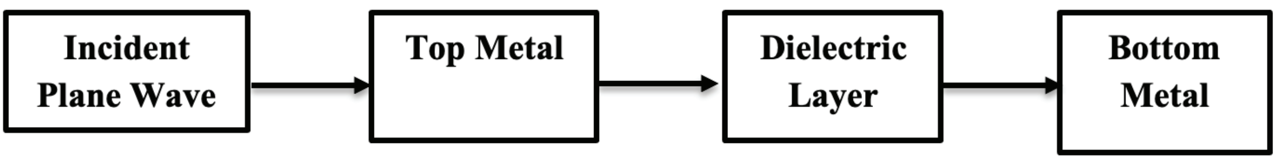

Figure 2. Basic block diagram of metasurface based perfect absorber.

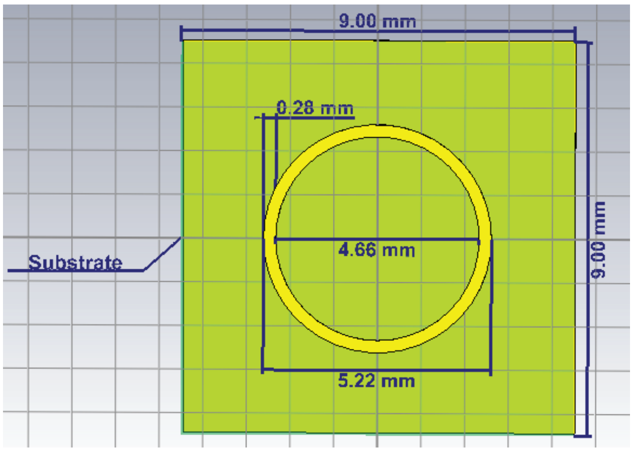

Figure 4. Design: 2 The geometry of the unit cell of the proposed metamaterial absorber with an inner ring.

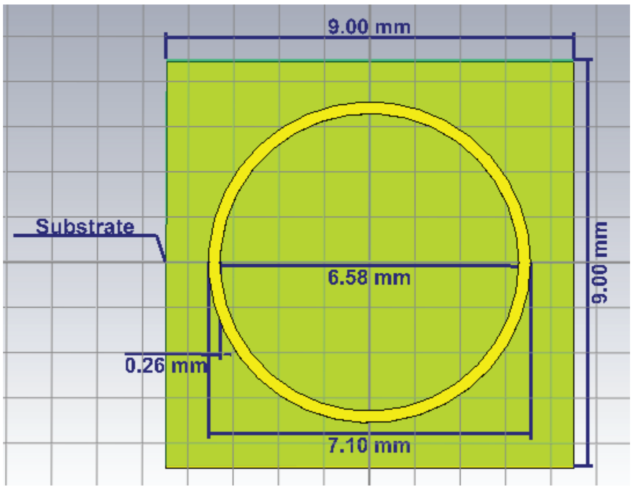

Figure 6. Design: 4 The geometry of the unit cell of the proposed metamaterial absorber with outer ring.

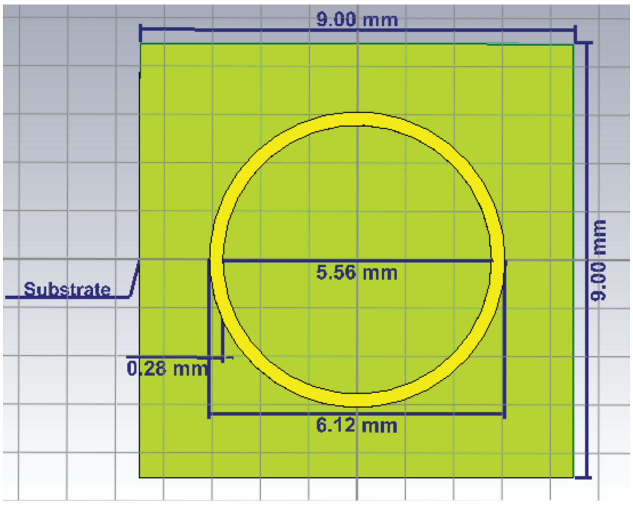

Figure 5. Design: 3 The geometry of the unit cell of the proposed metamaterial absorber with the middle ring.

Simulation

The simulation results for the triple circular ring metamaterial absorber with normal incident waves are presented in terms of high absorbance at three resonance frequencies indicated by f = 7.865 GHz, f = 9.855 GHz, and f = 11.445 GHz, and the corresponding absorbance are 96.62%, 78.668%, and 69.797%, respectively. The first, second, and third triple resonances are associated with the three smallest, medium, and biggest circular circles, respectively.

Figure 7 presents the absorbance values of the proposed metamaterial absorber for the TE-polarized incident wave obtained from simulations. The calculated resonant absorbance at resonant frequencies 7.865 GHz, 9.855 GHz, and 11.445 GHz are 96.62 %, 78.668 %, and 69.797 %. In so doing, the resonant frequencies remain almost constant, but there is a slight increase in the values; this occurs in the inner ring, in which case the resonances become 11.265 GHz with the corresponding absorbance levels as 96.32%

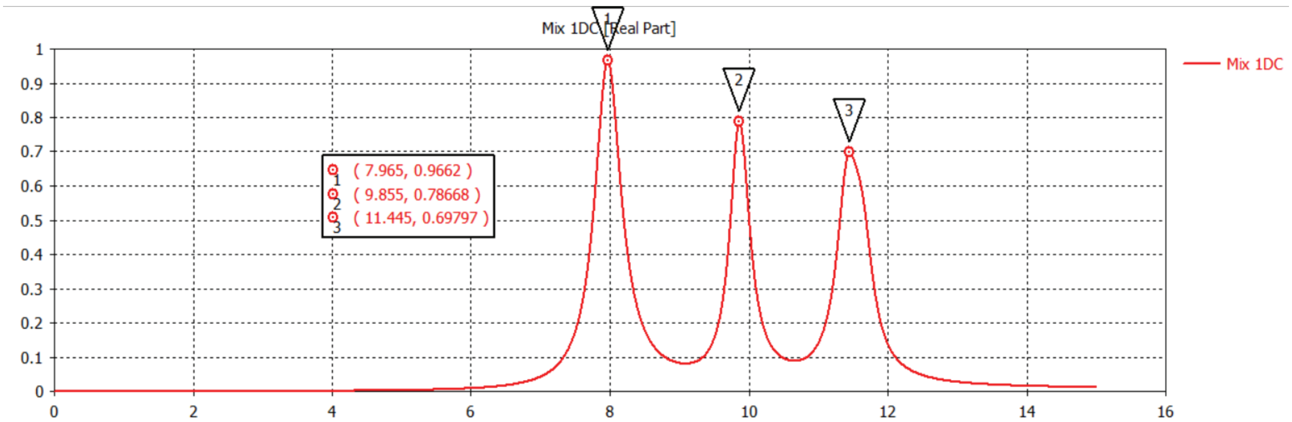

Figure 7. The frequency Vs absorption graph for design 1.

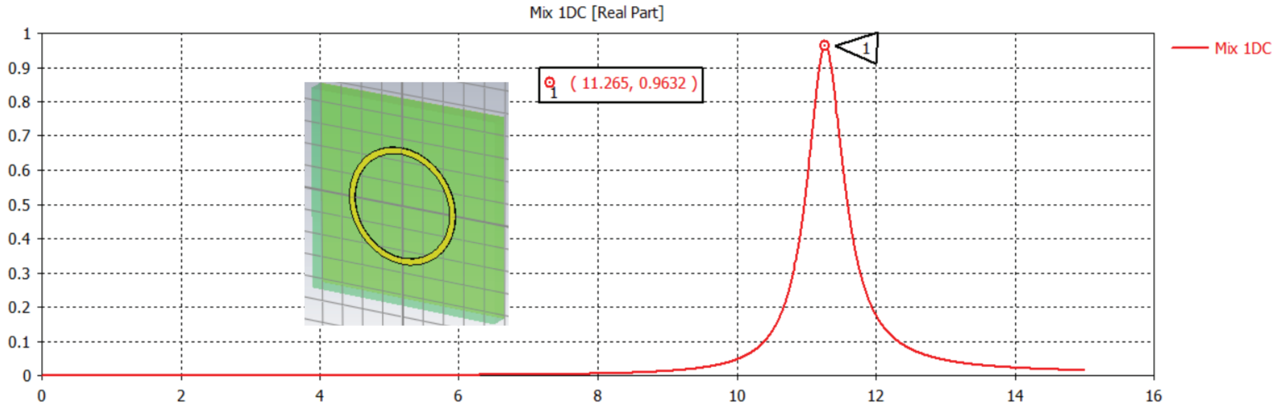

Figure 8. The frequency Vs absorption graph for design 2.

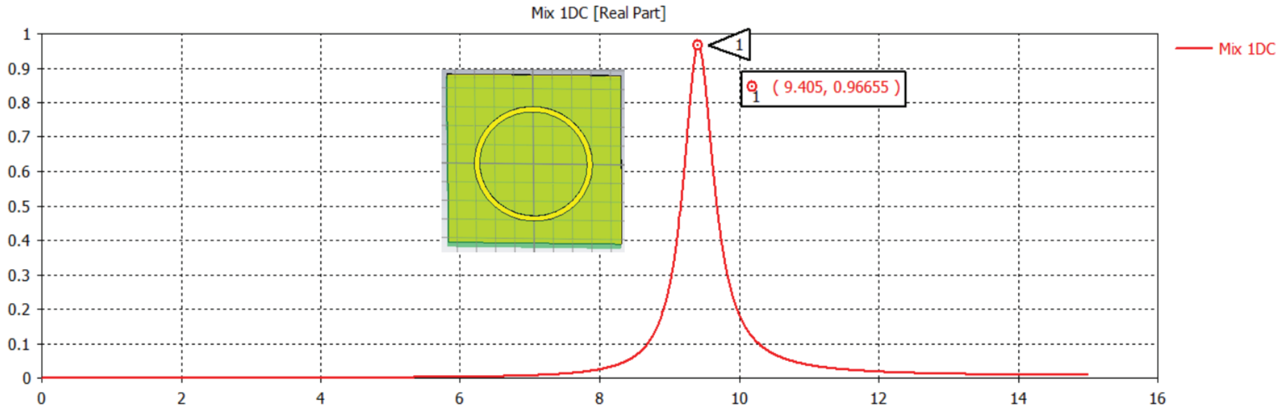

Figure 9. The frequency vs. absorption graph for design 3.

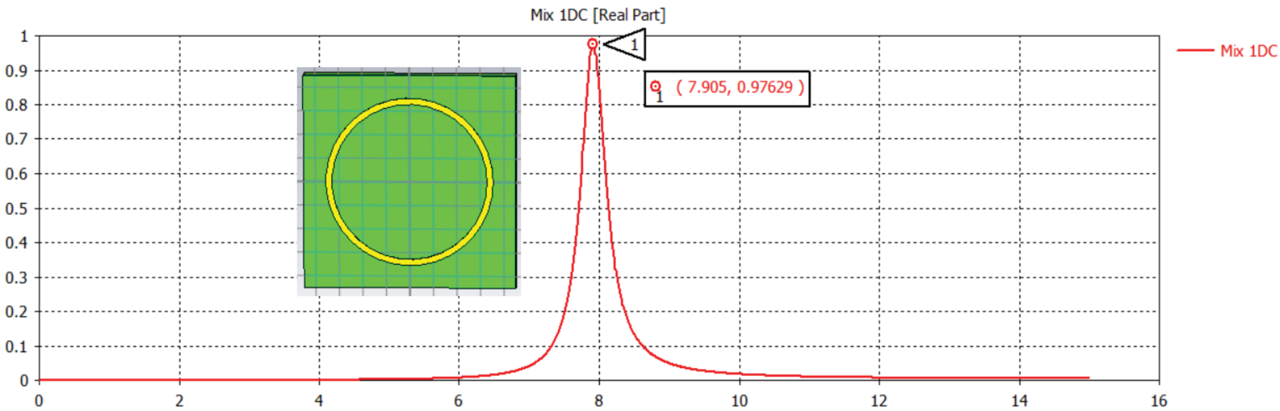

Figure 10. The frequency Vs absorption graph for design 4.

as shown in Figure 8. Similarly for middle ring subsequently the observed values of resonant frequencies are at 9.405 GHz along with the absorbance values are 96.655% as shown in Figure 9. At last, the measurement of resonant frequencies for outer ring is 7.905 GHz, and the absorbance level corresponding to Figure 10 is 97.629% with the help of outer ring.

Table 1 shows the results of a comparative analysis that was carried out to assess the influence that the incorporation of circular ring structures in the metamaterial had on

Table 1. Comparative analysis of four deigns

No. of rings	Frequency in GHz	Absorption in %
Inner ring	11.265	96.32
Middle ring	9.405	96.66
Outer ring	7.905	97.63
All rings	7.965	96.62
	9.855	78.67
	11.445	69.80

Table 2. Comparative Analysis of deigns 2, 3 & 4

No. of rings	Frequency in GHz	Absorption in %
Inner ring	10.52	84.28
Middle ring	7.23	88.23
Outer ring	6.9	95.56

the overall design. When the rings in the structure were raised, the investigation noted the occurrence of resonance frequency; the distinct frequency at which maximum absorption takes place as 7.965 GHz. Moreover, this specific design showed a high degree of absorbance with 96.62% marked as a number.

A simulation study has been performed to investigate the impact of changing the diameters of the three rings in a metamaterial absorber structure on the resonance frequency and absorption properties of the proposed metamaterial absorber structure by providing the observation results in Table 2.

FABRICATION AND MEASUREMENT

The selection of the dimensions for the three circular rings of the metamaterial absorber is achieved through simulation. The fabricated triple circular ring metamaterial absorber is 54 mm × 54 mm corresponding to a 6 × 6 array of triple circular ring elements and 90 mm × 90 mm corresponding to a 10 × 10 array of triple circular ring elements using copper metallic traces printed on an FR-4 dielectric substrate using a printed circuit board (PCB) [Figure respectively (Fig. 11, Fig. 12). The structure is then put under measurement to confirm its EM absorbing features. Details of the measurement setup are shown in Figure 13 and include a microwave anechoic chamber. There are two horn antennas located on the semi-circle track which can be adjusted to specific angles. These antennas are also connected to a vector network analyzer (VNA) at port 1 (input) and port 2 (output). These electromagnetic waves are emitted by the horn antenna at port 1 and are radiated onto the sample sheet, while the horn antenna at port 2 receives the reflected waves. The VNA will read the reflection magnitude on the sample sheet. In addition, a pyramidal microwave absorber surrounds the sample sheet to prevent unnecessary coupling of signals between the horn antennas. The transmitting and receiving horn antennas are connected with the VNA which measures reflection spectra from 1 GHZ to 15 GHZ. An aluminium board that is sectioned into two and acts as the ideal reference reflector is employed to calibrate the reflection measurement. For focusing only on reflection measurements, the metamaterial absorber sample is placed between four square aluminium plates of the same dimension – one square meter each. This structure helps to reduce transmission at all frequencies.

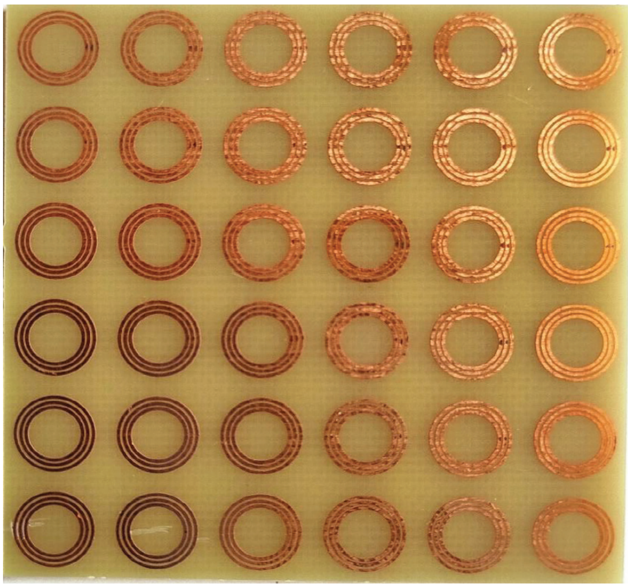

Figure 11. Fabricated 6 x 6 array.

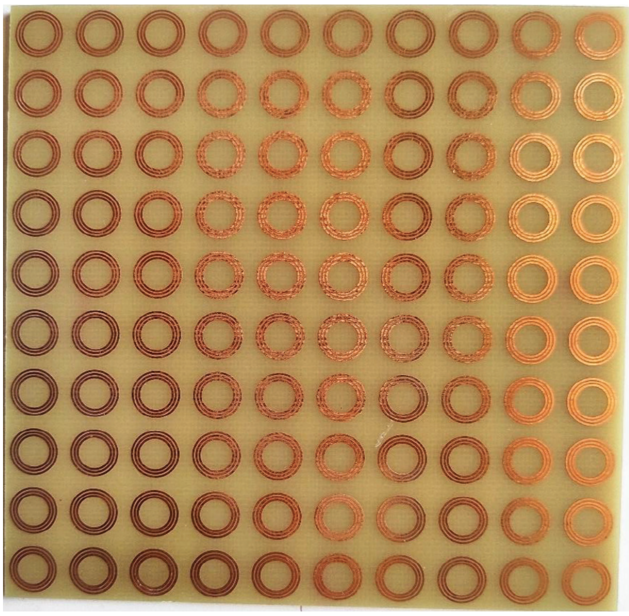

Figure 12. Fabricated 10 x 10 array.

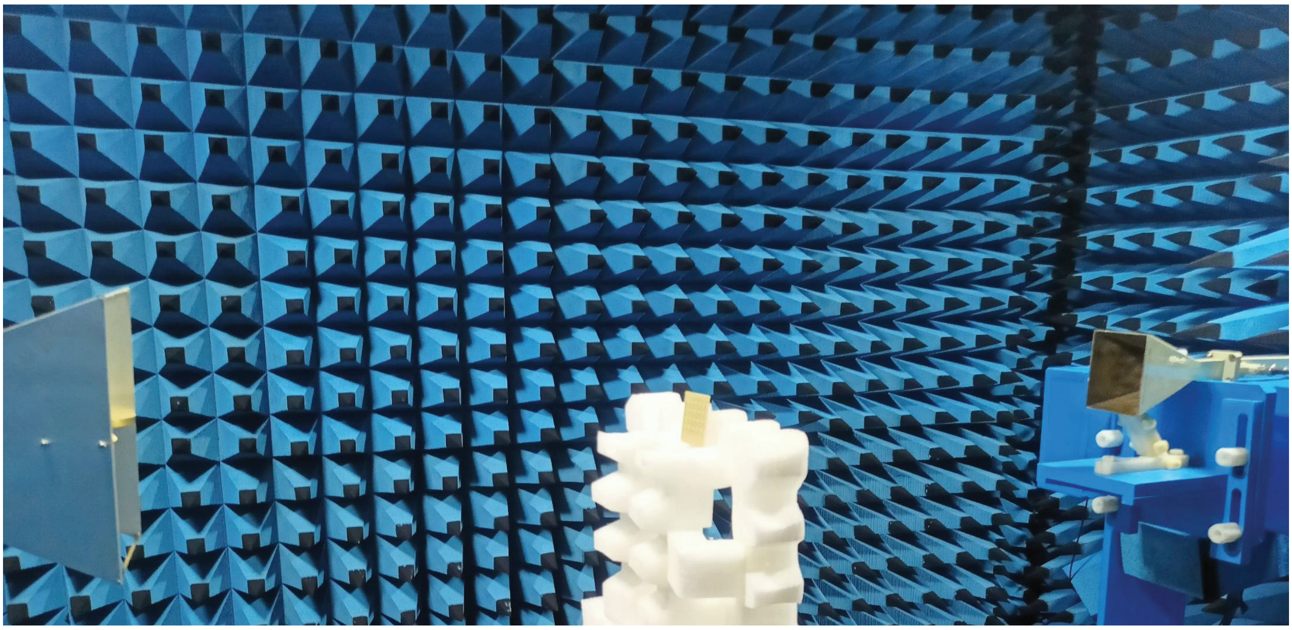

Figure 13. Experimental arrangement for validating the electromagnetic (EM) absorption properties of the metamaterial absorber.

Figure 14 and Figure 15 depict the measured EM absorbance of TE polarized wave under normal incidence for two arrays of 6 × 6 and 10 x 10, respectively. The experimental data tallies with the simulation result, for most of the cases, with some deviations. It should be noted that the described object has several resonance frequencies: 7. 832 GHz, 9. 596 GHz, and 11 GHz. When the operating frequency was set to 248 GHz, the calculated absorbance was 97. 802% of 77, 909% and 80. 351%, in that order. In the measurements, the above resonant frequencies are altered marginally to 7. 8 GHz, 9. 57 GHz, and 11.31 GHz having absorbance of 96. 78%; 76.28%; and 76%, 65%, respectively. Figure 14 and Figure 15 represent the measured values for 6x6 array and 10 × 10 array metamaterial absorbers with substrate 0.8 mm thickness of polyoxymethylene. Figure 16 and Figure 17 give the measured values for metamaterial

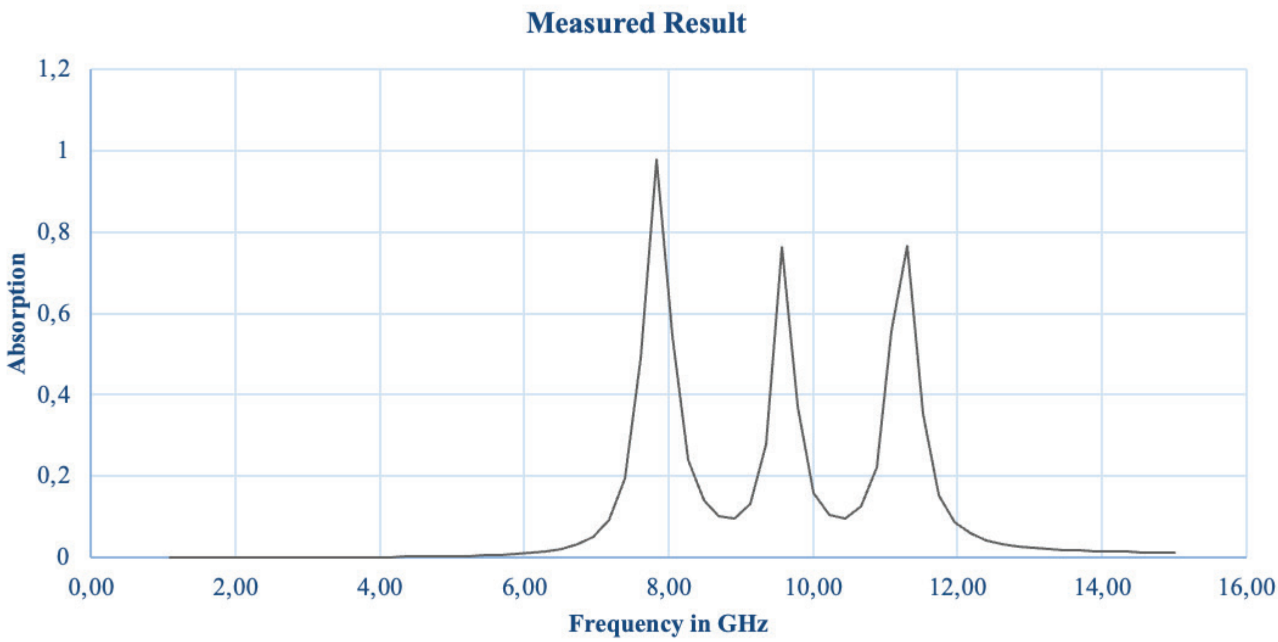

Figure 14. Measured Absorption (A) for 6x6 Array with thickness 0.8 mm.

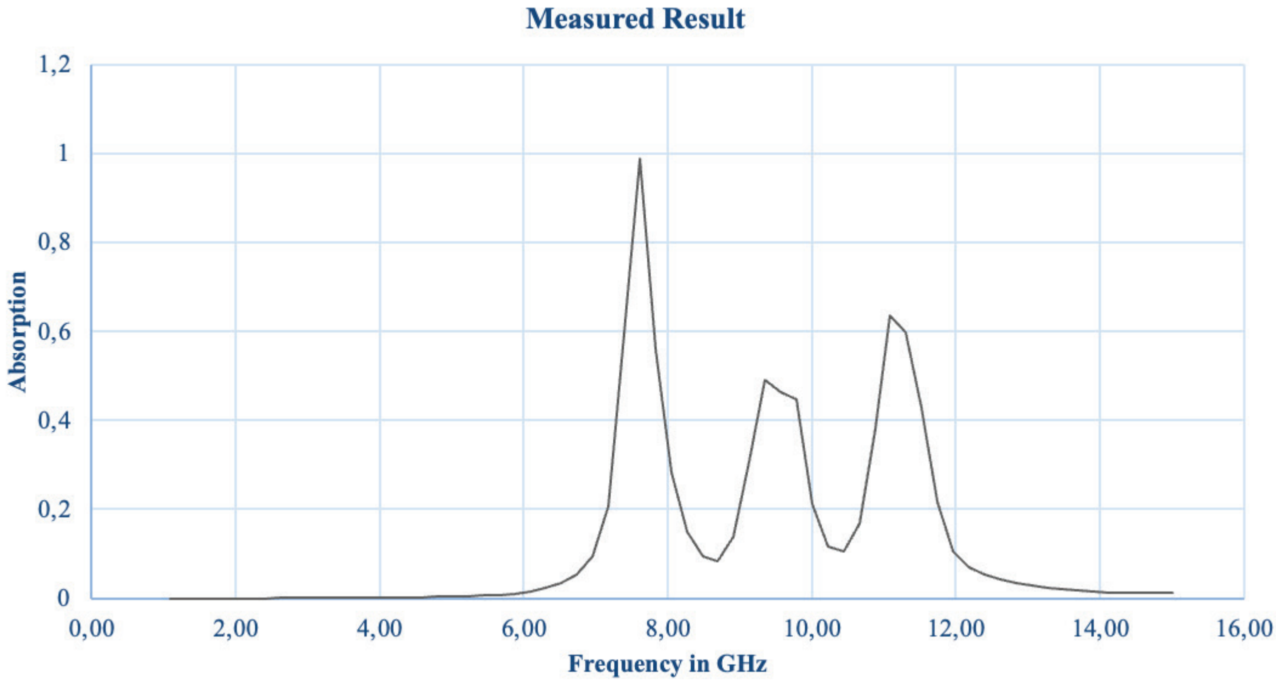

Figure 15. Measured Absorption (A) for 10x10 Array with thickness 0.8 mm.

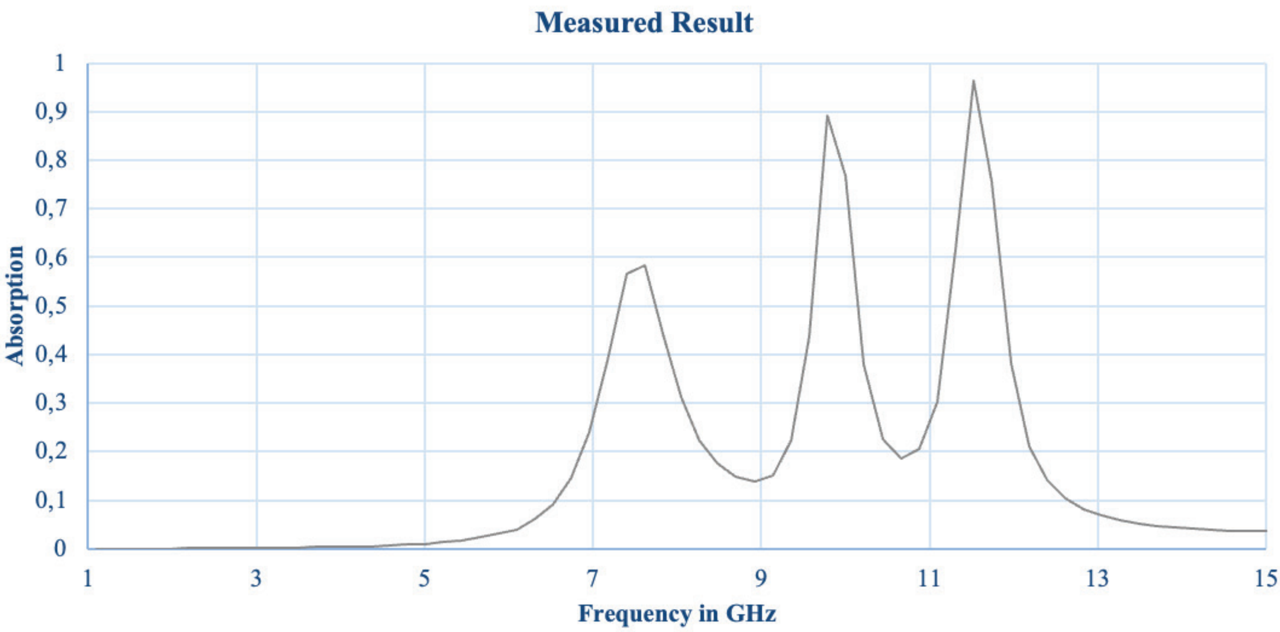

Figure 16. Measured Absorption (A) for 6x6 Array with thickness 1.6 mm.

absorbers with 6x6 array and 10x10 array structures with a 1. 6 mm thickness of the substrate. The values of absorbance obtained from the simulation results and the experiment agreed with each other to a minor degree which might be due to mutual coupling of the horn antennas and scattering from the structure. Tolerances in fabrication and dispersion of substrate dielectric also affect the frequency shift.

Two metamaterial absorbers, one with a 6x6 array and the other with a 10x10 array are fabricated using substrates of 0.8mm and 1.6mm thickness, respectively. Experimental measurements are carried out, and the outcomes are contrasted in Table 3. The comparative analysis of stimulated and measured results is shown in Table 4.

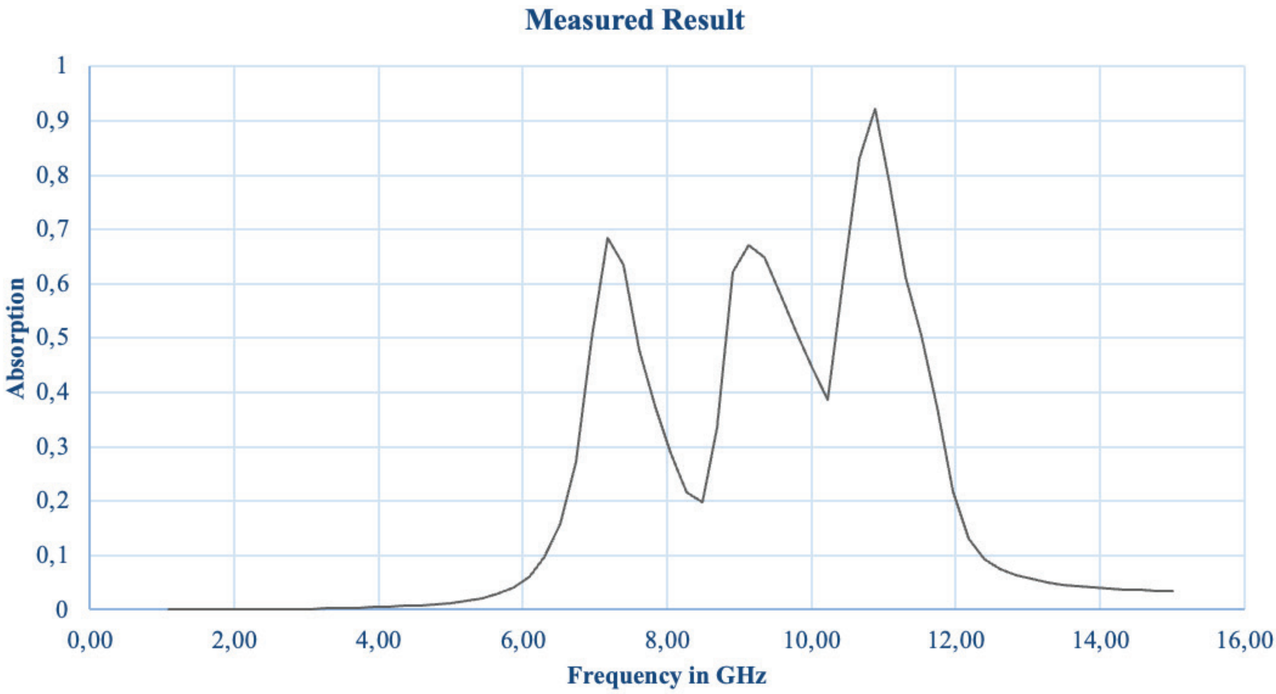

Figure 17. Measured Absorption (A) for 10x10 Array with thickness 1.6 mm.

Table 3. Comparative analysis with the thickness of the substrate

Thickness of Substrate	6 x 6 Array				10 x 10 Array			
	Simulated		Measured		Simulated		Measured	
	Freq. in GHz	Absorption in %	Freq. in GHz	Absorption in %	Freq. in GHz	Absorption in %	Freq. in GHz	Absorption in %
t = 1.6 mm	7.515	60.165	7.6	58.36	7.23	69.393	7.18	68.49
	9.87	99.04	9.78	89.09	9.05	68.89	9.14	67.03
	11.58	99.221	11.52	96.44	10.842	92.49	10.18	92.17
t = 0.8 mm	7.832	97.802	7.8	96.78	7.58	99.726	7.61	98.90
	9.596	77.909	9.57	76.28	9.4	49.61	9.35	49.23
	11.248	80.351	11.31	76.65	11.164	65.52	11.09	63.69

Table 4. Comparative Analysis of the proposed design

Ref.	Size (mm)	Frequency Range (GHz)	Design	Absorption (%)	Variation of Substrate Thickness (mm)	Array
[5]	10 x 10	5.376 10.32 12.25	a double E-shaped symmetric SRRs	Above 99%	No	No
[7]	35 x 32	1.21 3.64 5.30	a modified square-shape closed-loop resonator	94 % 90 % Above 99 %	No	No
Proposed design	9 x 9	7.515 9.87 11.58	Triple Circular Ring	60.17 Above 99 % Above 99 %	Yes t = 0.8 mm t = 1.6 mm	Yes 6 x 6 10 x 10

CONCLUSION

In conclusion, all steps connected with the design, fabrication, and evaluation of a triple circular ring metamaterial absorber have been completed. Moreover, a contribution towards understanding the relationship between the number of circular rings in the structure and the substrate thickness on absorbance has been made. The evaluation of the absorber is made in terms of absorbance and thickness of the substrate. Measured and simulated results also show fair comparison with small frequency shifts. Studies on the structural parameters of the triple circular ring metamaterial absorber are presented using analyses of the substrate thickness. Future research will focus on implementing structures that effectively work at high absorbance levels at multi-band frequencies without compromising at least 95% absorbance of the electromagnetic waves that hit them at right angles.

The strengths of this work are the high absorption of EM in three frequencies, the crystalline structure analysis at the atomic level, and the satisfactory match between the theoretical and the real model. Still, the drawbacks are found in the form of minor variations either in frequency or fabrication tolerance. Moreover, one can mention that subsequent research work should be devoted to improving the absorbance in other spectral regions, investigation of various materials and constructions, as well as, stability and effectiveness of PEF coatings in real conditions. Possible future studies like the development of absorbers for various angles of incidence and polarization, as well as the integration of absorber elements into actual goods. Further research on efficient manufacturing techniques is needed to encourage the use of the said absorbers. Discussions upon these kinds of challenges and novel trends can result in great advancements in the design of metamaterial absorbers where the present study facilitates the improvement of the given area of research.

AUTHORSHIP CONTRIBUTIONS

Authors equally contributed to this work.

DATA AVAILABILITY STATEMENT

The authors confirm that the data that supports the findings of this study are available within the article. Raw data that support the finding of this study are available from the corresponding author, upon reasonable request.

CONFLICT OF INTEREST

The author declared no potential conflicts of interest with respect to the research, authorship, and/or publication of this article.

ETHICS

There are no ethical issues with the publication of this manuscript.

STATEMENT ON THE USE OF ARTIFICIAL INTELLIGENCE

Artificial intelligence was not used in the preparation of the article.

REFERENCES

[1] Patel J, Mehta R. Simulation-based comparative review on a metasurface-based perfect absorber. J Adv Eng Comput 2023;7:204–209. [CrossRef]

[2] Jahan MI, Faruque MRI, Hossain MB. An X-shaped triple split ring resonator-based metamaterial perfect absorber with quad-band incident and polarization angle insensitivity for C, X, and Ku band applications. J Magn Magn Mater 2023:170940. [CrossRef]

[3] Jahan MI, Faruque MRI, Hossain MB, Khandaker MU, Elsayed F, Salman M, et al. Quad-band metamaterial perfect absorber with high shielding effectiveness using double X-shaped ring resonator. Materials 2023;16:4405. [CrossRef]

[4] Ullah N, Islam MS, Hoque A, Yong WH, Soliman MS, Islam MT. A compact-sized four-band metamaterial-based perfect absorber for electromagnetic energy harvesting applications. Opt Laser Technol 2024;168:109836. [CrossRef]

[5] Hossain MB, Faruque MRI, Islam MT, Singh M, Jusoh M. Triple band microwave metamaterial absorber based on double E-shaped symmetric split ring resonators for EMI shielding and stealth applications. J Mater Res Technol 2022;18:1653–1668. [CrossRef]

[6] Liu Z, Zhang J, Xu Z, Yuan Z, Mei Z, Niu T. Realization of an ultra-thin absorber with fragmented magnetic structure at L-, S-, and partial C-bands. J Appl Phys 2023;134. [CrossRef]

[7] Shahid M, Shanmuganantham T, Kumar SA. Metamaterial absorber for L-band, S-band, and C-band applications. Preprint 2023. [CrossRef]

[8] Jahan MI, Faruque MRI, Hossain MB, Abdullah S. An ultra-thin, triple-band, incident angle-insensitive perfect metamaterial absorber. Materials 2023;16:1623. [CrossRef]

[9] Ullah N, Islam MS, Hoque A, Yong WH, Soliman MS, Albadran S, et al. A compact complementary split ring resonator (CSRR) based perfect metamaterial absorber for energy harvesting applications. Eng Sci Technol Int J 2023;45:101473. [CrossRef]

[10] Rajyalakshmi G, Kumar YR, Krishna DR, Rao KS. Angle independent metamaterial absorber for S and C band application. Prog Electromagn Res C 2023;130:241–254. [CrossRef]

[11] Amer AAG, Sapuan SZ, Alzahrani A, Nasimuddin N, Salem AA, Ghoneim SSM. Design and analysis of polarization-independent, wide-angle, broadband metasurface absorber using resistor-loaded split-ring resonators. Electronics 2022;11:1986. [CrossRef]

[12] Hasan M, Islam MT, Almalki SHA, Alharbi AG, Alsaif H, Islam M, et al. Polarization insensitive dual band metamaterial with absorptance for 5G sub-6 GHz applications. Sci Rep 2022;12:1–20. [CrossRef]

[13] Hakim ML, Alam T, Almutairi AF, Mansor MF, Islam MT. Polarization insensitivity characterization of dual-band perfect metamaterial absorber for K band sensing applications. Sci Rep 2021;11:17829. [CrossRef]

[14] Hakim ML, Alam T, Islam MT, Baharuddin MH, Alzamil A, Islam MS. Quad-band polarization-insensitive square split-ring resonator (SSRR) with an inner Jerusalem cross metamaterial absorber for Ku- and K-band sensing applications. Sensors 2022;22:4489. [CrossRef]

[15] Kaur M, Singh HS. Design and analysis of a compact ultrathin polarization- and incident angle-independent triple band metamaterial absorber. Microw Opt Technol Lett 2020;62:1920–1929. [CrossRef]

[16] Deng G, Lv K, Sun H, Yang J, Yin Z, Li Y, et al. An ultrathin, triple-band metamaterial absorber with wide-incident-angle stability for conformal applications at X and Ku frequency band. Nanoscale Res Lett 2020;15:1–10. [CrossRef]

[17] Zhao G, Bi S, Cui Y. Study on the characteristics of a V-shaped metamaterial absorber and its application. AIP Adv 2019;9:075016. [CrossRef]

[18] Singh RK, Gupta A. A wrenched-square shaped polarization-independent and wide-angle stable ultra-thin metamaterial absorber for S-band, X-band and Ku-band applications. AEU Int J Electron Commun 2021;132:153648. [CrossRef]

[19] Naqvi SA, Baqir MA, Gourley G, Iftikhar A, Khan MS, Anagnostou DE. A novel meander line metamaterial absorber operating at 24 GHz and 28 GHz for the 5G applications. Sensors 2022;22:3764. [CrossRef]

[20] Shakiba L, Salehi MR, Emami F. A multiband perfect metamaterial absorber based on phase change material for switching and biosensing applications. Opt Commun 2024;560:130498. [CrossRef]

[21] Afsar MSU, Faruque MRI, Abdullah S, Hossain MJ. Rotational symmetric solar system shaped triple band perfect metamaterial absorber for S-, C-, and X-band application. Sens Actuators A Phys 2024;365:114839. [CrossRef]